Aug 24th, 12:00 AM - Aug 25th, 12:00 AM

Innovative Cross-section Shapes for Built-up CFS Columns. Experimental Investigation

Iveta Georgieva

Luc Schueremans

Lincy Pyl

Lucie Vandewalle

Twenty-First International Specialty Conference on Cold-Formed Steel Structures
St. Louis, Missouri, USA, October 24 & 25, 2012

Innovative cross-section shapes for built-up CFS columns. Experimental investigation

Iveta Georgieva[1], Luc Schueremans[2], Lincy Pyl[3], Lucie Vandewalle[4]

Abstract

Innovative cross-section shapes for built-up columns from cold-formed steel (CFS) profiles are evaluated experimentally. The goal is to obtain highly stable members with reduced sensitivity to bucking effects and initial imperfections, and therefore, higher strength-to-weight ratios. The columns have been designed following the principles of the direct strength method [1], with the ambition to exclude (or reduce) various buckling effects from the column response to compressive loads. Cross-section proportions and bolt spacing have been adapted, in order to interfere with the distortion of individual profiles and the overall buckling of the columns. Experiments show that, through proper design and insight into the behaviour of such members, columns with substantially increased overall capacity can be obtained. The good agreement between predicted and measured ultimate loads also indicates that such built-up assemblies could be integrated into everyday construction practice.

Introduction

Composed CFS elements are used in light steel framing, where higher loads need to be sustained. Their cross-section is usually symmetric, of higher strength and resistance against out-of-plane movement. Because the

[1] PhD Student, Catholic University Leuven, Heverlee, Belgium
[2] Associated professor, Catholic University Leuven, Heverlee, Belgium
[3] Associated professor, Free University of Brussels, Brussels, Belgium
[4] Head of the Building Materials and Technology Division at Catholic University Leuven, Heverlee, Belgium

production method remains unchanged, composed CFS members are a relatively cheap alternative to single profiles, which fail in overall buckling easily, if not laterally supported.
Buckling within a composed thin-walled element is not necessarily similar to the one observed in the individual components, when these are used alone. The additional support the profiles provide to each other can be used to design efficiently with CFS, if design guidelines are available.
Sixteen tests are performed on four proposed cross-section types. Each cross-section is bolted from three or four profiles of the standard shapes, widely available on the market (Σ, Z, channel or track). The profile geometry is optimised, in order to reduce buckling effects on local and global scale. Each cross-section type is tested in a single geometrical configuration and size, yet the type of connections at the ends of the member is varied – bolted or welded. The large number of tests is motivated by the desire to evaluate the scatter in the obtained resistances.
Comparison to EUROCODE-based calculations is presented, although the design of such members is outside the scope of the European standards. The latter underestimate the overall capacity of the members considerably, indicating that the rules, given in [2] and [3] are insufficient to estimate the capacity of such built-up assemblies.

Motivation for investigation

Built-up CFS members permeate the present-day construction practice, despite the lack of safe or accurate methodology for the design of these. The reliability of the predicted overall capacity then lies with the engineering judgement and experience of the designer.
A design method is needed that takes into account the important aspects in the behaviour of such members – The different types of buckling, sensitivities to imperfections and uncertainties, related to the material properties of CFS. The methodology should not depend on numerous cross-sectional properties, which cannot be determined for the built-up cross-section, unless full-scale tests are performed.
Previous investigations on built-up members (from Z-profiles, see [4] and [5]) showed, that alongside buckling, fastener flexibility also has a impact on the behaviour of the members, when these are interconnected by bolts and clearances are provided to ensure ease of assembly.

The performed investigation [6] shows that DSM could be extended towards composed members, if certain uncertainties are included in the interaction equations of DSM.

Cross-section shapes for built-up CFS profiles

The four profiles, used to assemble the proposed built-up shapes, are shown in Figure 1. These are dimensioned after examining buckling solutions, obtained from the open-source MATLAB code CUFSM [7]. The goal was to obtain section proportions, for which higher elastic buckling stress is obtained for local and distortional buckling. In this way, buckling effects can be reduced in the built-up assemblies. The four profiles are arranged into four composed sections, as shown in Figure 2.

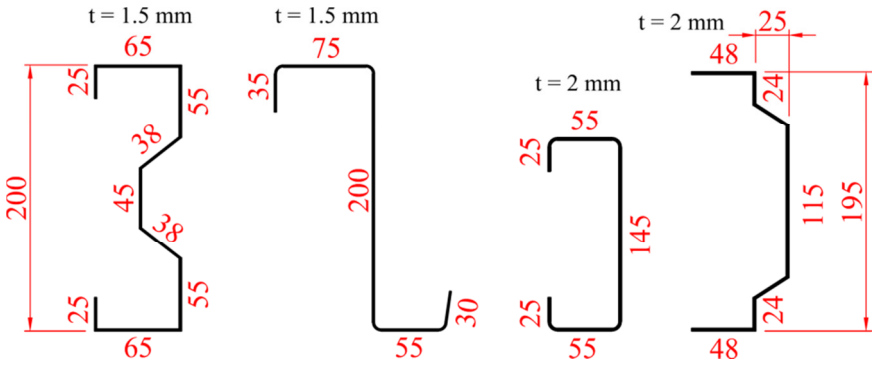

Figure 1. Profiles used to assemble the tested built-up members (Σ-, Z-, C- and track section)

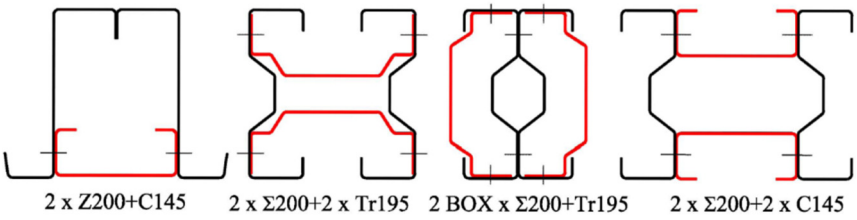

Figure 2. Built-up section types

The estimated capacity of the four single profiles, according to [2-3] and DSM, is listed and compared in Table 1. Similar resistances are obtained

according to the two standards. The buckling load-bearing capacity is evaluated for a length of 3 m and yield strength, equal to 390 N/mm^2 (nominal for steel grade S390). The larger capacity of the Z-section, when predicted by the European standards, is due to the assumed bending axes – the profile is designed for flexural buckling in the direction of the principal axes of the built-up cross-section. Slightly higher capacity is given by the DSM for the C-shape. This is explained by the interaction between the purely flexural and the torsional-flexural buckling modes, which occur at stresses 98.99 N/mm^2 and 101.13 N/mm^2, respectively. This interaction is not taken into account in the equations of DSM.

Table 1. Overall capacity of the individual profiles – EC3 vs. DSM

Section type	Design buckling resistance in compression, according to EN 1993 [2-3]		Nominal axial resistance, according to DSM [8]	
	Failure mode	$N_{b,Rd}$ [kN]	Failure mode	P_n [kN]
Z	Flexural Buckling	71.0[5]	Local buckling	35.14
Σ	Torsional Buckling	52.28	Overall buckling	51.85
C	Flexural Buckling / Torsional-Flexural Buckling	46.5	Overall buckling	49.85
Track	Torsional-Flexural Buckling	26.6	Overall buckling	26.97

If the built-up member capacity is to be estimated as the sum of the capacities of the individual profiles, the result will be over-conservative. The additional supports the profiles provide to each other can be responsible for a considerable increase in the elastic overall buckling stress. Also, bolting the profiles together along their length can successfully interfere with section distortion, increasing the distortional buckling stress 1.5 – 3.0 times [6].

To exclude from nine original proposals for built-up cross-section shapes [6], the full built-up sections are analysed in CUFSM. Several measures are taken in order to reduce buckling in the composed sections:

- Section proportion and wall thickness are adapted where needed;
- Edge or intermediate stiffeners are introduced where the stiffness is insufficient;

[5] Obtained for restrained bending parallel to built-up member axes

- Bolt-spacing is selected such as to interfere with the propagation of distortional buckling in the members;
- Bolts are placed in positions, where these could reduce both local and distortional buckling.

Special attention has been given to modelling the connection between the individual profiles in CUFSM. The profiles are interconnected at each bolt position, however, the longitudinal degrees of freedom are not altered, to allow for the effect of slip, due to bolt clearances, in the models [6].

After evaluating the initially proposed built-up cross-sections, four shapes are selected, based on three criteria:

- strength-to-weight ratio;
- buildability and ease of assembly;
- possibility to connect these to other elements or foundations.

The predicted buckling resistance according to DSM, when applied to build-up members, is listed in Table 2. The average ultimate capacity $N_{ult,av}$, measured during the tests, is also listed for comparison. The method gives a conservative prediction of the axial buckling resistance, and also indicates the type of buckling failure to be expected. Other failure modes, however, not caused by uniform axial compressive stress in the profiles, are not captured by the method. For example, plastic failure in the vicinity of connection pieces, due to large stress concentrations at the bolts, can cause premature failure, as seen with the 2xΣ200+2xTr195 specimens.

Table 2. Axial buckling resistances, obtained according to DSM

Section shape	Section area [mm^2]	Axial resistance P_n [kN]	Buckling type with minimal resistance	$N_{ult,av}$ [kN]
2xZ200+C145	1642.4	259.7[6] (151.4)	Local buckling	178.01
2xΣ200+2xTr195	2407.9	637.4	Local/Overall	593.29
2BOXxΣ200+Tr195	2407.9	223.9	Overall buckling	267.60
2xΣ200+2xC145	2240.4	454.2	Overall buckling	501.11

Due to the end connections configuration of the 2xZ200+C145 specimens, compressive loads are not directly applied to the C-shape. Strain gauge data also suggests that stress in the C-profile remains relatively low. The profile mainly serves to restrict distortion of Z-profiles, rather than take up

[6] Summed resistance of Z- and C- components of the cross-section

additional axial load. Also, 50x50 mm^2 openings are made in the C-section web, so that the bolts connecting the flanges to the Z-profiles can be fastened. Therefore, in Table 2, the resistance of this specimen is listed as 259.7 kN for the case when all profiles are loaded in uniform compression, and as 151.4 kN for the two Z-shapes only, with elastic buckling stresses obtained from the analysis of the built-up section.

Experiments

Sixteen tests are performed in compression to investigate the response of the build-up members and evaluate the scatter in axial resistance. Column bases are bolted at the ends in three of the four tests per section type, whereas the forth test is executed on a specimen with welded base plates.

Test set-up

A hydraulic press with fixed in the horizontal plane head and base is used to apply compression to the columns. Four displacement transducers (LVDTs) are placed at midheight to follow lateral movement; another LVDT is placed at the bottom connection, to measure accidental movement at the support. Four to nine strain gauges per specimen are glued at mid-height to measure axial strain. An optical device is used to record the initial imperfections and displacements at additional points in five of the tests.
The base plates at the column ends are used to transfer axial load to the specimens. The tests are displacement controlled, with a loading speed of 0.3 mm/min. In this way the post ultimate response of the columns can also be measured. The friction at the base plates keeps the columns in position.

Specimens

All columns are 3.0 m long, with section height 200 mm. Each specimen is assembled with base connections at the ends, as in actual buildings. The specimens are small, so that they can be assembled and handled in the lab easily. Bolts are 12 mm in diameter, class 8.8 (acc. to EN 1993-1-8), bolt holes have a diameter 13 mm. Not all bolts are accessible from both sides. In order to fasten the bolts between the profiles of the 2BOXxΣ200+Tr195 specimens, the nuts are pre-welded on one side through spot welding.

Specimens with welded base plates are also investigated, in order to assess the effect of restrained warping at the column ends on the ultimate capacity. Moreover, in this way the stiffness of the column will not be influenced by slip in the end connection pieces.
Previous investigations by the authors have shown that initial imperfections may have a very detrimental effect on the ultimate capacity built-up CFS members attain during experiments [4]. Such members are often longer, hence more slender on a global scale. Depending on the amplitude of initial deflections, for example, the resistance may vary 10-25% (in comparison to the average measured resistance), see [4]. On the other hand, if the columns are shorter or laterally braced, imperfections of shorter wavelength may show to be more important.
The built-up members, presented in this paper, have been designed to be less prone to buckling effects. Such members should be less sensitive to initial imperfections and the large scatter in the experimentally obtained resistance should be reduced.

Welded specimens

Specimens with welded base plates are tested, in order to (1) investigate the effect of restricting warping at the column ends, and (2) compare the response of a column, in which slip (due to clearances) in the end connections is eliminated, to the response of columns with bolted end connections, as such primary members are built in practice. Because primary CFS members usually have a higher thickness (2.0 – 5.0 mm) in building of larger scale, self-drilling screws cannot be used as a universal connector. Instead, producers opt for bolts. Bolts are the most common fastener, used in the Belgian engineering practice, to connect primary CFS members to each other or to foundations.
When welding the end plates (thickness 15 mm), precautions need to be taken to ensure that these two plates are parallel, to avoid eccentricity in the test set-up. The displacement of the hydraulic press head, applied to the columns to reach ultimate load, remains in the range 8 – 10 mm for welded specimens. Therefore, if the plates are not parallel, even deviations of 1-2 mm can influence the results significantly. With long specimens, the task of welding the two plates to be parallel becomes much more difficult.

In the presented test campaign, an attempt is made to eliminate the mentioned eccentricity. Nevertheless, due to the large initial imperfections in CFS built-up members [9], and the large length, the results are not perfect. This can be concluded after investigating the measured strains on the mid-height cross-section. In Table 3, the strains at 75% of the ultimate load are listed, to give an idea of the amount of eccentricity for each of the welded specimens. The gauges placement is given in Figure 3.

Table 3. Strains at 75 % of ultimate load [microstrain]

Cross-section	SG1	SG2	SG3	SG4	SG5	SG6	SG7	SG8	SG9
2xZ200+C145	782	1374	748	534	827	567	-	-	-
2xΣ200+2xTr195	761	886	933	1017	1175	1063	912	921	1054
2xΣ200+2xC145	981	1130	910	1157	965	1701	969	1086	-

The higher strain, measured by strain gauge 6 (SG6) for specimen 2xΣ200+2xC145 is explained by pronounced plastic local buckling in the C-section web. Nonetheless, this specimen shows the lowest eccentricity, followed by the 2xΣ200+2xTr195 and 2xZ200+C145 specimens.

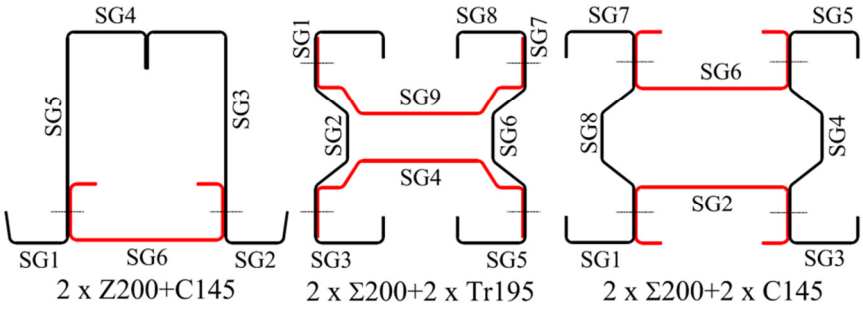

Figure 3. Strain gauge positions for welded specimens (at mid-heigth)

Experimental results

The measured ultimate capacity is listed in Table 4, alongside the primary failure mechanism, observed for the type of cross-section. Resistances, comparable to the predicted, are attained by the specimens, except for specimen type 2xΣ200+2xTr195. These columns fail prematurely, as a result of stress concentrations in the vicinity of connection pieces. This failure mode was first observed in a numerical model, which predicted an ultimate load of 596 kN, and a failure mechanism, as shown in Figure 5c.

Table 4. Experimental results – ultimate loads and failure modes

Section shape	Test No	$N_{ult,EXP}$ [kN]	$N_{ult,av}$ [kN]	Δ [%]	Prevailing failure mode
2xZ200+C145	1	170.20	178.01	4.39	Local buckling in Z-profiles (web and flanges). Less pronounced distortion in the Z- and C-profiles.
	2	180.66		1.49	
	3	183.18		2.91	
	welded	305.59	305.59	-	Local buckling in Z- (web and flanges) and C-profiles. Less pronounced distortion in the Z- and C-profiles.
2xΣ200+2xTr195	1	591.03	593.29	0.38	Plastic deformation at the end connections, due to stress concentrations; plastic local buckling in track sections.
	2	580.63		2.13	
	3	608.19		2.51	
	welded	600.97	600.97	-	Distortional-global buckling interaction
2BOXxΣ200+Tr195	1	279.40	267.60	4.41	Plastic deformation at the end connections (cross-section reduced to 2xΣ-sections). Limited lateral movement in test 2.
	2	255.79		4.41	
	3	232.64*		*Test not completed	
2xΣ200+2xC145	1	510.95	501.11	1.96	Plastic deformation at the end connections; plastic local buckling in the webs of C-profiles.
	2	489.49		2.32	
	3	502.89		0.36	
	welded	588.98	588.98	-	

Where: $$\Delta = \frac{N_{ult,EXP} - N_{ult,av}}{N_{ult,av}}$$ Eq. 1

Yet, no adaptations were made to the connection pieces to prevent this premature failure. Excluding the described failure mode would require that heavier connection pieces be produced (with higher bolt pitch), which would make these harder to handle in laboratory conditions.
The scatter in the obtained resistances remains low. Ultimate capacities remain within 5% of the average loads (see Table 4 and eq.1). All specimens fail in localised effects, which results in a subsequent snap-through and yielding.

Failure modes

The failure modes, observed during the experiments are shown in Figure 4 to Figure 7 for the four built-up column types.

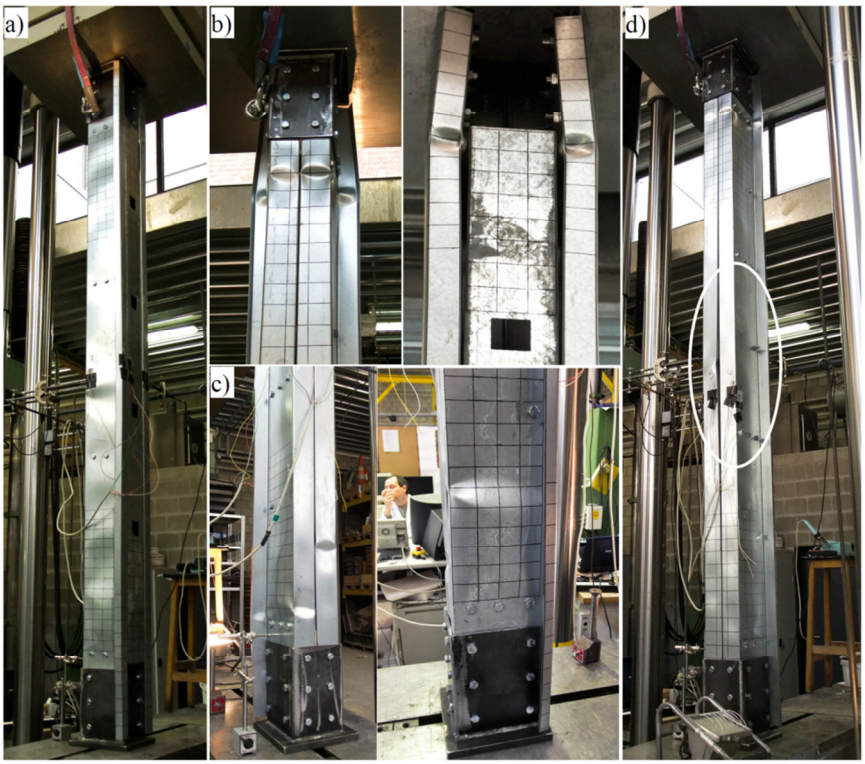

Figure 4. 2xZ200+C145 - failure mechanisms: a) local buckling; b) at top connection piece; c) at bottom connection piece; d) distortion in Z-sections.

The 2xZ200+C145 columns fail in local buckling in the slender webs and large flanges (width 75 mm) of the Z-profiles. After considerable plastic deformation has occurred in the Z-shapes, separation of the cross-section is caused by distortion of the C-section at its ends, Figure 4b. Distortion of the large flanges of the Z-sections (where these are in contact) happens after the ultimate capacity has been reached.

The welded specimen of this type fails in local buckling, in this case also in the C-shape. Because 50x50 mm^2 holes are provided in the C-section web, local buckling remains limited to the column ends and does not spread along the column length.

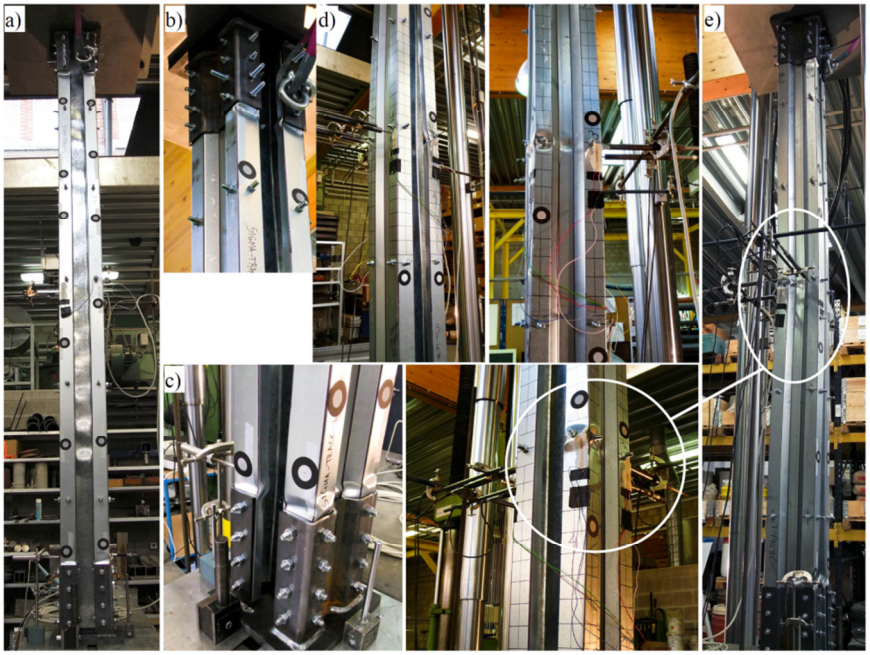

Figure 5. 2xΣ200+2xTr195 – failure mechanisms: a) overall deformation and plastic local buckling in the track profiles; b) and c) plastic deformation at connection pieces; d) distortion and yielding at midheight; e) overall deformation due to distortion at mid-height.

The 2xΣ200+2xTr195 specimens are at their ultimate load when large deformations appear at the connection pieces. Shortly before that, plastic local buckling had appeared in the webs of the track profiles, which

remains there after disassembling the columns. Distortion in the Σ-shapes, followed by yielding at midheight, result in lateral movement of the specimen. The welded specimen fails without end deformations. Distortion of the Σ-sections in the column mid-region leads to the onset of lateral movement, at which point the ultimate load is reached. After reconsidering results, obtained from CUFSM, the authors suggest a further study to investigate the overall-distortional buckling interaction in this section type.

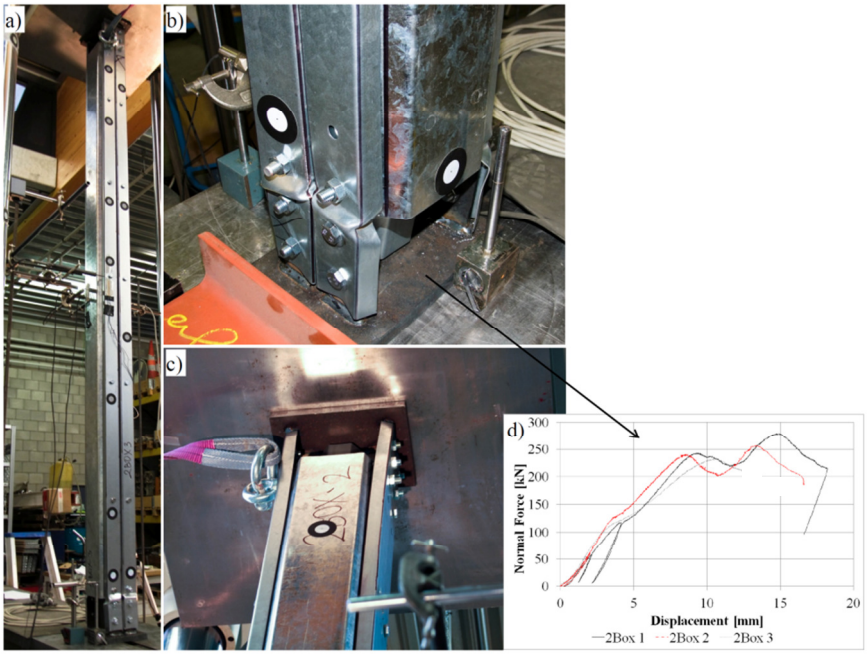

Figure 6. 2BOXxΣ200+Tr195- failure mechanisms: a) overall deformation; b) plastic zones at the connections; c) onset of deformations at connections.

The failure of the 2BOXxΣ200+Tr195 columns is triggered at the connections. Due to the abrupt change in cross-sectional area, plastic regions are formed, as shown in Figure 6b. This stage in the response history of the columns corresponds to the first peak in the normal force vs. applied longitudinal displacement diagram, shown in Figure 6d. After the column has settled into another stable configuration, the load continues to increase, until the ultimate load is reached.

The failure mode at the ends can be restricted (postponed) by providing a restraint against warping at the ends. Figure 6c shows the formation of plastic regions at its onset – distortion of the flanges of the Σ-shapes happens due to lack of longitudinal restraint at the very ends of the profiles.

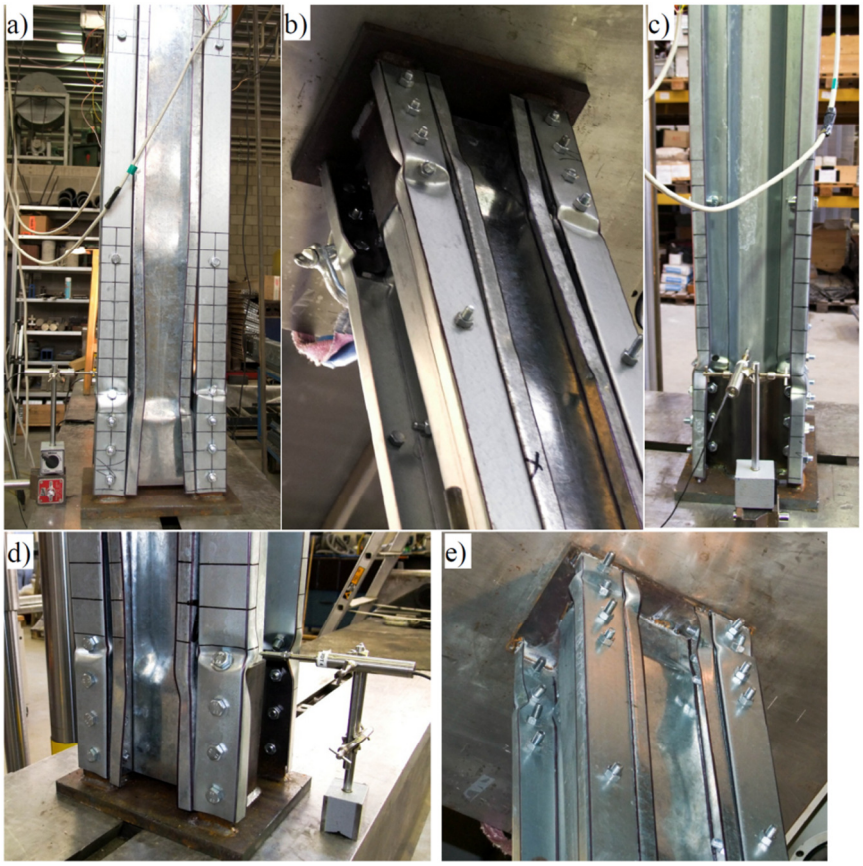

Figure 7. 2xΣ200+2xC145 failure mechanisms: a) distortion of C-section and plastic deformation at bottom base; b) top base; c) distortion in Σ-shape; d) deformation at bottom base; e) deformation in welded specimen.

Specimen type 2xΣ200+2xC145 fails via plastic regions at the end connections, see Figure 7. Distortion of the C-shape can be seen in Figure 7a and d, at the level of the first bolt hole. Limited distortion in the Σ-sections appears after the ultimate load has been reached. The failure mode

of the welded columns of this type is shown in Figure 7e. Local buckling in the C-section web also appears, alongside yielding.

Welded specimen

The experiments suggest that welding base plates at the built-up column ends can result in a notable increase in the overall axial capacity and reduced flexibility of the member. Figure 8 shows the response-history of two of the section types – bolted and welded specimens are compared.

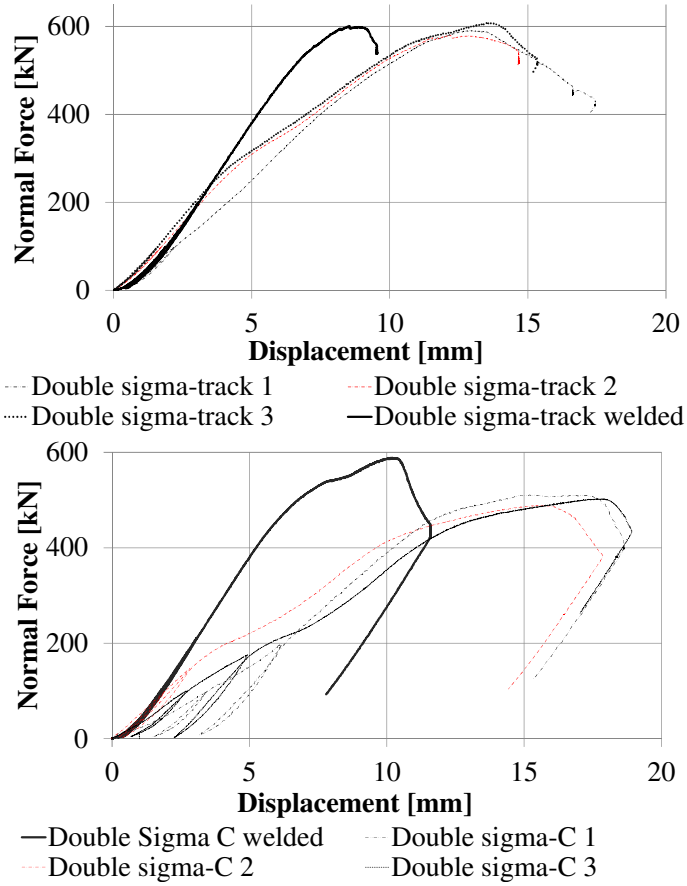

Figure 8. Load vs. axial displacements: a) 2xΣ200+2xTr195; b) 2xΣ200+2xC145.

Conclusions

The equations of the direct strength method are used to predict the overall axial capacity of built-up members from CFS profiles. The elastic buckling stresses are obtained from analysis of the built-up sections in CUFSM [7]. Based on the predictions of the method, cross-section shapes are optimised in order to obtain members of higher strength-to-weight ratios. By proper choice of profile geometry and fastener positions, members with significantly increased overall capacity are obtained. To confirm, 15 tests are performed on four built-up section types. The method gives a good prediction of the experimentally obtained overall capacity of the columns.

[1] B.W. Schafer, Review: The Direct Strength Method of cold-formed steel member design, J Const Steel Res 64, 7-8 (2008) 766-778.
[2] EN 1993-1-3:2006. Eurocode 3: Design of steel structures, Part 1–3: Supplementary rules for cold-formed thin gauge members and sheeting.
[3] EN 1993-1-1:2005. Eurocode 3: Design of steel structures, Part 1-1: General rules and rules for buildings, 2005.
[4] I.B. Georgieva, L. Schueremans, L. Pyl, Experimental investigation of built-up double-Z members in bending and compression, Thin Wall Str 53, 4 (2012) 48-57.
[5] I.B. Georgieva, L. Schueremans, L. Pyl, Composed columns from cold-formed steel Z-profiles. Experiments and code-based predictions of the overall resistance, Engineering Structures 37, 4 (2012) 125-134.
[6] I. Georgieva, Design of innovative built-up members from cold-formed steel profiles, Internal report, Catholic University Leuven, 2011
[7] Z. Li, B.W. Schafer, Buckling analysis of cold-formed steel members with general boundary conditions using CUFSM: conventional and constrained finite strip method, 20th Internaltional Specialised Conference on Cold-Formed Steel Structures, St. Louis, Missouri, USA, (2010),
[8] North American Specification for the Design of Cold-Formed Steel Structural Members, 2007.
[9] I.B. Georgieva, L. Schueremans, L. Pyl, L. Vandewalle, Numerical investigation of built-up double-Z members in bending and compression, Thin-Walled Structures (2012, submitted)

Notation

$N_{b,Rd}$ Design buckling resistance in compression according to [3]
P_n Nominal axial strength, according to [8]
$N_{ult,EXP}$ Experimentally obtained member capacity (single tests)
$N_{ult,av}$ Average experimentally obtained member capacity